

Thermochromic Luminescence of Sol–Gel Films Based on Copper Iodide Clusters

Cédric Tard,[†] Sandrine Perruchas,^{*,†} Sébastien Maron,[†] Xavier F. Le Goff,[‡] François Guillen,[§] Alain Garcia,[§] Jacky Vigneron,^{||} Arnaud Etcheberry,^{||} Thierry Gacoin,[†] and Jean-Pierre Boilot^{*,†}

Laboratoire de Physique de la Matière Condensée (PMC) and Laboratoire Hétéroéléments et Coordination (DCPH), CNRS, Ecole Polytechnique, 91128 Palaiseau Cedex, France, Institut de Chimie de la Matière Condensée de Bordeaux (ICMCB), CNRS, 87 Avenue du Docteur A. Schweitzer, 33608 Pessac Cedex, France, and Institut Lavoisier de Versailles (ILV), UMR CNRS 8180, Université de Versailles Saint Quentin, 45 Avenue des Etats-Unis, 78035 Versailles Cedex, France

Received June 30, 2008. Revised Manuscript Received September 5, 2008

The incorporation of copper iodide clusters in sol–gel silica has been investigated to prepare materials with original luminescent properties. The synthesis, structural characterizations, and optical properties of sol–gel films containing $[\text{Cu}_4\text{I}_4\text{L}_4]$ clusters, L = phosphine-based ligands, are reported. Clusters studied are $[\text{Cu}_4\text{I}_4(\text{PPh}_2(\text{CH}_2)_2\text{Si}(\text{OCH}_2\text{CH}_3)_3)_4]$ (**C1**), able to copolymerize with the silica matrix, and $[\text{Cu}_4\text{I}_4(\text{PPh}_2(\text{CH}_2)_2\text{CH}_3)_4]$ (**C2**) used as a reference for the characterizations. The luminescent films exhibit the optical properties of these clusters in accordance with XPS and NMR studies demonstrating their integrity in the gel matrix. The temperature dependence of light emission properties of clusters and films shows, for the first time for phosphine-based $[\text{Cu}_4\text{X}_4\text{L}_4]$ clusters, thermochromic luminescence with bright yellow luminescence at room temperature and purple emission at 77 K. As a result of weak Cu–Cu interactions, the two emissive states appear as highly coupled with a low energy barrier ($2 \text{ kJ} \cdot \text{mol}^{-1}$), leading to a controlled thermochromism in a large temperature range.

Introduction

Research on luminescent materials has been actively pursued in the last two decades due to their numerous applications in light emitting devices (fluorescent tubes, lasers, cathode X-ray, projection television, OLED, flat panel display, etc.). Silica- and/or siloxane-based hybrid organic–inorganic matrices present several advantages to design materials for optical applications such as mild synthesis conditions, versatile chemistry, easy shaping, good mechanical properties, and excellent optical quality.^{1–3} For applications in solid-state lasers⁴ or electroluminescent devices,⁵ numerous luminescent transparent composite materials (films or monoliths) have been prepared by dispersing or grafting

luminescent species in sol–gel silica matrices.⁶ Organic dyes,⁷ nanoparticles, such as semiconductor quantum dots,⁸ and rare-earth doped oxides,⁹ and also coordination complexes of lanthanide ions^{10–13} generally constitute the active luminescent species trapped in these sol–gel materials. In the near future, luminescent transition metal clusters could represent another class of phosphors for the synthesis of light-emitting materials (silica-based materials or not). These molecular clusters are promising photoactive species since they combine inorganic nature of nanoparticles with monodisperse size distribution and easy functionalization of organic molecules.

Photoluminescent d^{10} coinage metal compounds have been studied for many years due to their various photophysical luminescent properties.^{14–16} Among them, the formulated

* Corresponding authors. Fax: (+33) (0)1 69 33 47 99. Phone: (+33) (0)1 69 33 46 51. E-mail: sandrine.perruchas@polytechnique.edu (S.P.); jean-pierre.boilot@polytechnique.fr (J.-P.B.).

[†] Laboratoire de Physique de la Matière Condensée (PMC).

[‡] Laboratoire Hétéroéléments et Coordination (DCPH).

[§] Institut de Chimie de la Matière Condensée de Bordeaux (ICMCB).

^{||} Université de Versailles Saint Quentin.

- (1) (a) Brinker, C. J.; Scherrer, G. W. *Sol-Gel Science The Physics and Chemistry of Sol-Gel Processing*; Academic Press: San Diego, CA, 1990. (b) Avnir, D.; Levy, D.; Reisfeld, R. *J. Phys. Chem.* **1984**, *88*, 5956.
- (2) (a) Sanchez, C.; Ribot, F. *New J. Chem.* **1994**, *18*, 1007. (b) Schubert, U.; Hüsing, N.; Lorenz, A. *Chem. Mater.* **1995**, *7*, 2010. (c) Loy, D. A.; Schea, K. J. *Chem. Rev.* **1995**, *95*, 1431.
- (3) Pénard, A.-L.; Gacoin, T.; Boilot, J.-P. *Acc. Chem. Res.* **2007**, *40*, 895.
- (4) Faloss, M.; Canva, M.; Georges, P.; Brun, A.; Chaput, F.; Boilot, J.-P. *Appl. Opt.* **1997**, *36*, 6760.
- (5) de Morais, T. D.; Chaput, F.; Boilot, J.-P.; Lahilil, K.; Darracq, B.; Lévy, Y. *Adv. Mater. Opt. Electron.* **2000**, *10*, 69.

- (6) Sanchez, C.; Lebeau, B.; Chaput, F.; Boilot, J.-P. *Adv. Mater.* **2003**, *15*, 1969.

- (7) Avnir, D.; Braun, S.; Lev, O.; Levy, D.; Ottolenghi, M. *Sol-Gel Optics, Processing and Applications*; Klein, L. C., Ed.; Kluwer Academic Publishers: Dordrecht, 1994; p 539.

- (8) (a) Epifani, M.; Leo, G.; Lomascio, M.; Vasaneli, L.; Manna, L. *J. Sol-Gel Sci. Technol.* **2003**, *26*, 441. (b) Lifshitz, E.; Dag, I.; Litvin, I.; Hodes, G.; Gorer, S.; Reisfeld, R.; Zelnor, M.; Minti, H. *Chem. Phys. Lett.* **1998**, *288*, 188.

- (9) Buisette, V.; Giaume, D.; Gacoin, T.; Boilot, J.-P. *J. Mater. Chem.* **2006**, *16*, 529.

- (10) Armelao, L.; Bottaro, G.; Quici, S.; Cavazzini, M.; Raffo, M. C.; Barigelletti, F.; Accorsi, G. *Chem. Commun.* **2007**, 2911.

- (11) Qi, W.; Li, H.; Wu, L. *Adv. Mater.* **2007**, *19*, 1983.

- (12) Lenaerts, P.; Storms, A.; Mullens, J.; D'Haen, J.; Görrler-Walrand, C.; Binnemas, K.; Driesen, K. *Chem. Mater.* **2005**, *17*, 5194.

- (13) Raehm, L.; Mehdi, A.; Wickleder, C.; Reyé, C.; Corriu, J. P. *Chem. Mater.* **2007**, *19*, 12636.

- (14) Barbieri, A.; Accorsi, G.; Armaroli, N. *Chem. Commun.* **2008**, 2185.

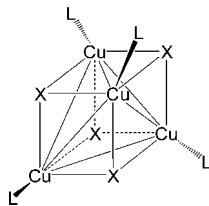


Figure 1. General representation of $[\text{Cu}_4\text{X}_4\text{L}_4]$ clusters ($\text{X} = \text{Cl}, \text{Br}, \text{I}$; L = pyridine or amine-based derivatives).

tetra-copper(I) clusters $[\text{Cu}_4\text{X}_4\text{L}_4]$ ($\text{X} = \text{Cl}, \text{Br}, \text{I}$; L = pyridine or amine-based derivatives) are known to be highly luminescent at room temperature.^{15,17} The molecular structure of these cubane type clusters is represented Figure 1. These compounds are easily synthesized in solution and can be obtained with different types of ligands (L) allowing their functionalization. Besides, these copper clusters display emission spectra that are strikingly sensitive to their environment, the temperature, and the rigidity of the medium. For example, the thermochromic luminescence¹⁸ originates from two emission bands whose relative intensities vary in temperature.¹⁹ At room temperature, the luminescence is dominated by a low energy band (LE) which has been attributed, based on experimental data¹⁵ and recent DFT calculations,²⁰ to a combination of a halide-to-metal charge transfer (XMCT) and copper-centered $d \rightarrow s, p$ transitions. This emission is called “cluster centered” (^3CC) as it involves a $[\text{Cu}_4\text{I}_4]$ cluster centered triplet excited state, which is essentially independent of the nature of the ligand. At low temperature, this band is extremely weak, and the emission is dominated by a higher energy band (HE) which has been attributed to a triplet halide-to-pyridine ligand charge-transfer ($^3\text{XLCT}$) excited state. As the π^* orbitals of the ligands are involved in this XLCT band, the emission at low temperature is only observed for clusters incorporating π -unsaturated ligands. All these properties make these copper clusters particularly attractive for their incorporation in organic or inorganic polymeric matrices, to synthesize materials with original optical applications. To our knowledge no such cluster-based materials have been already reported.

There have been considerably less photophysical investigations of $[\text{Cu}_4\text{X}_4\text{L}_4]$ clusters with L = phosphine derivatives compared to pyridines or amines ones. The only luminescence studies reported for clusters with the $[\text{Cu}_4\text{I}_4]$ core have concerned the emission at 654 nm of $[\text{Cu}_4\text{I}_4(\text{P}^n\text{Bu}_3)_4]$ ¹⁵ at room temperature in toluene and of $[\text{Cu}_4\text{I}_4(\text{dmpp})_4]$ ($\text{dmpp} = 1\text{-phenyl-3,4-dimethylphosphole}$)^{21,22} at 15 K in the solid state at 664 nm. By analogy with $[\text{Cu}_4\text{I}_4\text{L}_4]$ (L = pyridine or amine derivatives) clusters, this emission observed for $[\text{Cu}_4\text{I}_4(\text{P}^n\text{Bu}_3)_4]$ was attributed to the LE band previously cited (XMCT/ $d-s$). The absence of the HE band

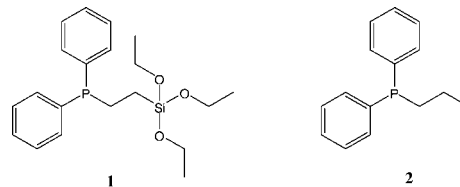


Figure 2. Phosphine ligands studied: **1** = $\text{PPh}_2(\text{CH}_2)_2\text{Si}(\text{OCH}_2\text{CH}_3)_3$, **2** = $\text{PPh}_2(\text{CH}_2)_2\text{CH}_3$.

was explained by the saturated aliphatic character of the P^nBu_3 ligand. For $[\text{Cu}_4\text{I}_4(\text{dmpp})_4]$, the emission was assigned to a metal–ligand charge-transfer transition (MLCT) based on vibronic structure analyses. No luminescence properties at low temperature have been reported for these two compounds.

Herein, we report on the synthesis, structural characterizations, and optical properties of sol–gel films containing $[\text{Cu}_4\text{I}_4\text{L}_4]$ clusters. Iodide cluster derivatives were selected because of their known higher luminescence quantum yield and stability compared to the chloride and bromide analogues.¹⁵ An original copper iodide cluster with phosphine ligands bearing alcoxysilane groups is synthesized allowing a covalent grafting of clusters to the silica matrix. Since luminescence properties of $[\text{Cu}_4\text{I}_4\text{L}_4]$ clusters having phosphine ligands are not well-known, a reference cluster without polymerizable groups is also prepared to facilitate the characterization of films. Thus, the cluster integrity in sol–gel films is demonstrated from XPS and NMR studies. Light emission properties of clusters and films are studied in detail as a function of the temperature. The thermochromic luminescence is observed for the first time in sol–gel films. Under UV excitation, clusters and films exhibit a bright yellow luminescence at room temperature, while the emission becomes purple after immersion in liquid nitrogen. Moreover, we clearly display the high coupling between excited states ($^3\text{XLCT}$ and ^3CC) with the appearance of two thermally equilibrated emissions in the 10–120 K range.

Experimental Section

Synthesis. All manipulations were performed with standard air-free techniques using Schlenk equipment, unless otherwise noted. Solvents were distilled from appropriate drying agents and degassed prior to use. Diphenyl-ethyltriethoxysilane-phosphine (**1**) was synthesized by the method reported in the literature.²³ Copper(I) iodide, diphenyl-propyl-phosphine (**2**), and methyltriethoxysilane (MTEOS) were purchased from Aldrich and used as received.

C1-2. To a suspension of CuI in dichloromethane (20 mL) was added the corresponding ligand (**1** or **2**) (Figure 2). The solution was stirred for 2 h at room temperature. The mixture was filtrated, and after evaporation of the solvent the product was recovered as colorless oil for **C1**. **C2** was purified by flash chromatography (silica gel, cyclohexane/ethylacetate 4:1), and colorless crystals were obtained by slowly cooling the cyclohexane/ethylacetate solution from room temperature to 4 °C. **C1**: CuI (1.0 g, 5.3 mmol), **1** (2.0 g, 5.3 mmol), yield = 72% (2.2 g, 0.95 mmol). **C2**: CuI (840 mg, 4.4 mmol), **2** (1 g, 4.4 mmol), yield = 76% (1.4 g, 3.3 mmol). Elemental analyses and NMR characterization are reported in Supporting Information.

- (15) Ford, P. C.; Cariati, E.; Bourassas, J. *Chem. Rev.* **1999**, 99, 3625.
- (16) Yam, V. W.-W.; Lo, K. K.-W. *Chem. Soc. Rev.* **1999**, 28, 323.
- (17) Vitale, M.; Ford, P. C. *Coord. Chem. Rev.* **2001**, 219, 3.
- (18) Hardt, H. D.; Pierre, A. Z. *Anorg. Allg. Chem.* **1973**, 402, 107.
- (19) Kyle, K. R.; Ryu, C. K.; DiBenedetto, J. A.; Ford, P. C. *J. Am. Chem. Soc.* **1991**, 113, 2954.
- (20) De Angelis, F.; Fantacci, S.; Sgamellotti, A.; Cariati, E.; Ugo, R.; Ford, P. C. *Inorg. Chem.* **2006**, 45, 10576.
- (21) Lai, D. C.; Zink, J. I. *Inorg. Chem.* **1993**, 32, 2594.
- (22) Attar, S.; Bowmaker, G. A.; Alcock, N. W.; Frye, J. S.; Bearden, W. H.; Nelson, J. H. *Inorg. Chem.* **1991**, 30, 4743.

- (23) Bunlaksananusorn, T.; Knochel, P. *Tetrahedron Lett.* **2002**, 43, 5817.

C1 Films. The sol was prepared by mixing **C1** cluster, methyltriethoxysilane (MTEOS), *N,N*-dimethylformamide, and HCl aqueous solution (pH = 2.5) with a molar ratio of 1.5×10^{-3} :1:3:3. The mixture was stirred at room temperature overnight. The solvents were evaporated until the volume of the solution was reduced by 80% and a viscous liquid was obtained. After filtration a colorless and transparent liquid was obtained which was diluted by a factor of 2 with tetrahydrofuran and spin-coated on substrates at room temperature (3000 rpm, 2 min). Films obtained were colorless with thickness typically of 500 nm to 1 μ m. The substrates (glass, silica, silicon) were previously soaked in a piranha solution, washed with water and ethanol, and dried.

Characterizations. ^1H and ^{31}P liquid-state NMR spectra were recorded on Bruker AvanceII300 or Tecmag Apollo360 spectrometers, respectively, using Bruker probes at room temperature, operating at the radio frequency of 300 MHz (for ^1H) and 145 MHz (for ^{31}P). ^1H spectra were internally referenced from peaks of residual protons in deuterated solvents or from tetramethylsilane (TMS). A solution of 85 wt % H_3PO_4 was used as an external standard for ^{31}P spectra. Elemental analyses (C, H) were performed by the Service Central d'Analyses, CNRS of Vernaion. UV–visible absorption and transmittance spectra were recorded with a Varian Cary 50 spectrophotometer on films deposited on quartz substrates.

Luminescence spectra were recorded on a SPEX Fluorolog FL 212 spectrofluorimeter (HORIBA JOBIN YVON). The excitation source is a 450 W xenon lamp; excitation spectra were corrected for the variation of the incident lamp flux, as well as emission spectra for the transmission of the monochromator and the response of the photomultiplier (Peltier cooled Hamamatsu R928P photomultiplier). Low temperature measurements have been done with two different setups: a liquid nitrogen cryostat Meric TR S1900 or a liquid helium circulation cryostat SMC TBT Air Liquid model C102084. Determinations of the quantum luminescence yield for clusters and films are described in Supporting Information.

XPS spectra were recorded on a Thermo Electron VG-ES-CALAB 220 iXL spectrometer. Films were coated on p^+ silicon wafer. X-ray excitation was performed with a twin anode using its Al $\text{K}\alpha$ line. This excitation mode was preferred to a monochromatic one to minimize the charging effect. So spectra were recorded without any charge compensation by an electron flood gun. Presented data were recorded in a constant energy analyzer mode with pass energy of 20 eV. The photoelectrons were detected perpendicularly to the surface. The samples were stable under long time experiments. Spectrometer calibration was performed using the manufacturer procedure and was completed by a self-consistent check, on sputtered copper, silver, and gold samples, based on the ASTM E902-94 recommendation. Binding energy values of Au $4f_{7/2}$ and Cu $2p_{3/2}$ were 84 and 932.65 eV, respectively. The atomic % compositions are obtained using the peak areas of the levels corrected by the respective sensitivity factors. A global correction of the binding energy (BE) positions was performed assuming a pure Cu(I) contribution and shifting Cu $2p_{3/2}$ lines to 933 eV, the value reported for the $[\text{Cu}_4\text{Cl}_4(\text{PPh}_3)_4]$ cluster.²⁴

Single crystals suitable for X-ray structure determination were obtained for **C2** as described in the synthesis section. Crystals were mounted on fiberglass using paraton oil and immediately cooled to 150 K in a cold stream of nitrogen. All data were collected on a Nonius Kappa CCD diffractometer at 150(1) K using Mo $\text{K}\alpha$ ($\lambda = 0.71073$ Å) X-ray source and a graphite monochromator. The cell parameters were initially determined using more than 50

reflections. Experimental details are described in Table S1 (Supporting Information). The crystal structures were solved in SIR 97²⁵ and refined in SHELXL-97²⁶ by full-matrix least-squares using anisotropic thermal displacement parameters for all non-carbon and non-hydrogen atoms. All the hydrogen atoms were placed in geometrically calculated positions.

Results and Discussion

Synthesis and Structural Characterization of Clusters and Films. $[\text{Cu}_4\text{I}_4\text{L}_4]$ clusters coordinated by pyridine or amine-based ligands have been extensively studied compared to other ligands. However, the synthesis of sol–gel silica films requires the use of an aqueous solution of HCl as catalyst, and pyridine and amine-based complexes are known to be unstable in acidic conditions. Therefore, iodide clusters are functionalized with phosphine derivatives, which are known to be more stable.

The functional cluster (**C1**) is synthesized with the $[\text{Cu}_4\text{I}_4]$ moiety coordinated by a diphenyl-phosphine ligand bearing a trialkoxysilane group formulated $\text{PPh}_2(\text{CH}_2)_2\text{Si}(\text{OCH}_2\text{CH}_3)_3$ (**1**) and represented in Figure 2. Ligands bearing alcoxysilane groups are used to copolymerize with silica precursors of the matrix during the sol–gel reactions. This leads to a covalent grafting of clusters to the silica network and to high concentration and homogeneous distribution of clusters within the matrix (see XPS measurements). Cluster **C1** is prepared as colorless oil. The ^1H NMR spectrum shows that a small portion of alcoxysilane groups are hydrolyzed, probably explaining negative attempts of crystallization for this cluster.

Compounds based on transition metals with d^{10} electronic configuration are known to present a variety of structural forms. Although the most commonly observed structure for 1:1:1 Cu:X:L stoichiometry is the tetranuclear motif $[\text{Cu}_4\text{X}_4\text{L}_4]$, it is important to verify the molecular structure of **C1** to correctly analyze the optical properties of the corresponding materials. Thus, to ascertain the cubane molecular structure of cluster **C1**, a “reference” cluster was synthesized. This reference cluster **C2** was obtained by using the ligand $\text{PPh}_2(\text{CH}_2)_2\text{CH}_3$ (ligand **2** in Figure 2) which differs from **1** by the absence of alcoxysilane group. As for **C1** and in the same conditions, the reaction of **2** with CuI leads to the corresponding clusters $[\text{Cu}_4\text{I}_4(\text{2})_4]$ (**C2**). **C2** was crystallized, and its structure was solved by single crystal X-ray diffraction analysis at 150 K. The molecular structure of **C2** is depicted in Figure 3.

As expected, **C2** presents the cubane structure formed by four copper atoms and four iodine atoms which occupy alternatively the corners of a distorted cube. More precisely, the $[\text{Cu}_4\text{I}_4]$ core consists in a copper tetrahedron embedded within a somewhat larger iodine tetrahedron. The phosphine ligands (**2**) are bonded to each copper atom by the phosphorus atom. **C2** is thus formulated $[\text{Cu}_4\text{I}_4(\text{PPh}_2(\text{CH}_2)_2\text{CH}_3)_4]$ in agreement with NMR and elemental analysis. The values

(24) Battistoni, C.; Mattogno, G.; Paparazzo, E. *Inorg. Chim. Acta* **1985**, *102*, 1.

(25) Altomare, A.; Burla, M. C.; Camalli, M.; Cascarano, G.; Giacovazzo, C.; Guagliardi, A.; Moliterni, A. G. G.; Polidori, G.; Spagna, R. *J. Appl. Crystallogr.* **1999**, *32*, 115.

(26) Sheldrick, G. M. *SHELXL-97*; Universität Göttingen: Göttingen, Germany, 1997.

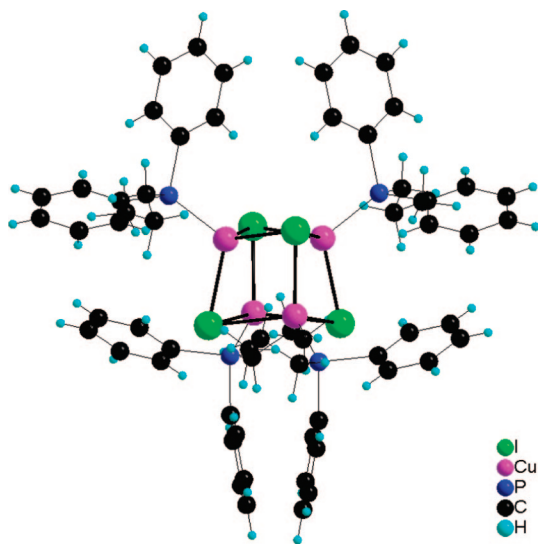


Figure 3. Molecular structure of **C2** [$\text{Cu}_4\text{I}_4(\text{PPh}_2(\text{CH}_2)_2\text{CH}_3)_4$].

for the Cu–I (2.668 and 2.701 Å) and Cu–P (2.254 Å) distances are within the range of reported values for this type of cluster with phosphine ligands such as PPh_3 ²⁷ and PPh_2CH_3 .²⁸ In **C2**, the Cu–Cu bonds lengths are 3.079 and 3.265 Å. These values are slightly longer compared to those found in similar clusters [$\text{Cu}_4\text{I}_4(\text{PPh}_3)_4$] (average 2.968 Å, range 2.839–3.165 Å at 295 K) and [$\text{Cu}_4\text{I}_4(\text{PPh}_2\text{CH}_3)_4$] (average 2.930 Å, range 2.840–3.010 Å at 295 K). The Cu–Cu bonds in [$\text{Cu}_4\text{I}_4\text{L}_4$] clusters based on pyridine or amine ligands are significantly shorter compared to phosphine derivatives.²⁹ For example, in [$\text{Cu}_4\text{I}_4\text{py}_4$] Cu–Cu bond distances are in the range 2.619–2.721 Å (average 2.690 Å),³⁰ that is, shorter than the sum of the van der Waals radii of copper(I) (2.80 Å),³¹ implying high metal–metal bonding interactions.

By comparing the different analyses of clusters **C1** and **C2** (NMR, luminescence vide infra), it can be assumed that the structure of **C1** has a cubane form as expected for the stoichiometry employed. Moreover, as already mentioned, poor literature data are available concerning the optical properties of [$\text{Cu}_4\text{X}_4\text{L}_4$] clusters with L = phosphine ligands. The **C2** cluster obtained as a colorless solid has helped the characterization of the luminescent properties of **C1** and the corresponding sol–gel films.

C1 was incorporated within a sol–gel silica matrix by using MTEOS (methyltriethoxysilane) as silica precursor. The copolymerization was performed by classical sol–gel process in acidic conditions. The gel obtained was spin-coated on substrates leading to transparent and colorless films (**C1** film).

To know whether all the clusters are conserved after the sol–gel process, we have performed NMR and X-ray photoelectron spectroscopy (XPS) experiments. ³¹P liquid NMR spectra of the sol before spin coating show a singlet centered at –24.9 ppm and a less intense one at +36.8 ppm

(Figure S3, Supporting Information). The major peak at –24.9 ppm corresponds to the phosphorus atom coordinated to copper atoms of the cluster. The second peak at +36.8 ppm corresponds to oxidized phosphorus, so to the ligand $\text{OPPh}_2(\text{CH}_2)_2\text{Si}(\text{OC}_2\text{H}_5)_3$. On the basis of several experiments, the proportion of the two species [$\text{Cu}(\text{PPh}_2(\text{CH}_2)_2\text{Si}(\text{OC}_2\text{H}_5)_3)$]: $\text{OPPh}_2(\text{CH}_2)_2\text{Si}(\text{OC}_2\text{H}_5)_3$ deduced from the peak area values is around 10:1. The reactions were also performed under inert atmosphere (nitrogen), but the proportion of oxidized ligands did not decrease. The oxidation of the ligand can be explained by the use of HCl to generate the acidic conditions required to the catalysis of the sol–gel reactions. Similar observations have been previously reported when this ligand is bound to silicon.³²

XPS measurements were performed on the **C2** cluster and **C1** films, and the corresponding data are reported in Table 1. Survey spectra detect only the expected atomic elements: Cu, I, P, O, Si, and C, supporting a very clean and reproducible coating procedure. As expected, a 1:1:1 Cu:I:P stoichiometry is observed for the cluster **C2**. In contrast with NMR results, the **C1** film appears as slightly substoichiometric in phosphorus (vide infra). Measurements on several samples gave similar atomic Si/Cu ratios confirming homogeneous distribution of clusters in the silica matrix. This Si/Cu ratio is low compared to the starting composition (15 instead of 170). This is probably due to the filtration of the sol before deposition, which eliminates some silica aggregates. As clearly suggested by the direct binding energy (BE) data (Table 1), the spectra are slightly shifted toward positive BE, indicating a slight charging effect. This charging effect is evidenced through the asymmetric shape of the XPS peaks as shown for the Cu 2p ones in Figure 4. In accordance with XPS report concerning the [$\text{Cu}_4\text{Cl}_4(\text{PPh}_3)_4$] cluster giving Cu 2p_{3/2} binding energy at 933 eV,²⁴ a global BE correction has been performed (see Table 1 and Experimental Section).

The I 3d signals present only one contribution in agreement with only one chemical environment. They are similar in shape and position for **C2** cluster and **C1** film (Figures S5–6, Supporting Information). If we consider the correction of the charging effect describe in Table 1, the BE positions become very close for **C2** and **C1** samples (619.72 and 619.63 eV, respectively) consistent with I(–I) species.³³ The P 2p signals are also similar for **C2** cluster and **C1** film (Figures S5–6, Supporting Information). After correction, their BEs have very specific positions around 131.3–131.5 eV. These typical values are consistent with one phosphorus species corresponding to the phosphine ligand coordinated to copper atoms. Our values are in perfect agreement with the XPS data reported for the [$\text{Cu}_4\text{Cl}_4(\text{PPh}_3)_4$] cluster (131.5 eV).²⁴ Phosphorus oxide observed by NMR was not detected by XPS analysis (a phosphorus oxide must appear at 133 eV without the charging effect). This shows a problem on the phosphorus measurement which is probably related to the substoichiometry found and could be due to a change of

(27) Dyason, J. C.; Healy, P. C.; Engelhardt, L. M.; Pakawatchai, C.; Patrick, V. A.; Raston, C. L.; White, A. H. *J. Chem. Soc., Dalton Trans.* **1985**, 831.

(28) Churchill, M. R.; Rotella, F. J. *Inorg. Chem.* **1977**, 16, 3267.

(29) Vega, A.; Saillard, J.-Y. *Inorg. Chem.* **2004**, 43, 4012.

(30) Raston, C. L.; White, A. H. *J. Chem. Soc., Dalton Trans.* **1976**, 2153.

(31) Bondi, A. J. *Phys. Chem.* **1964**, 68, 441.

(32) Komoroski, R. A.; Magistro, A. J.; Nicholas, P. P. *Inorg. Chem.* **1986**, 25, 3917.

(33) *X-ray Photoelectron Spectroscopy Database 20*, Version 3.0; National Institute of Standards and Technology: Gaithersburg, MD (<http://srdata.nist.gov/XPS>).

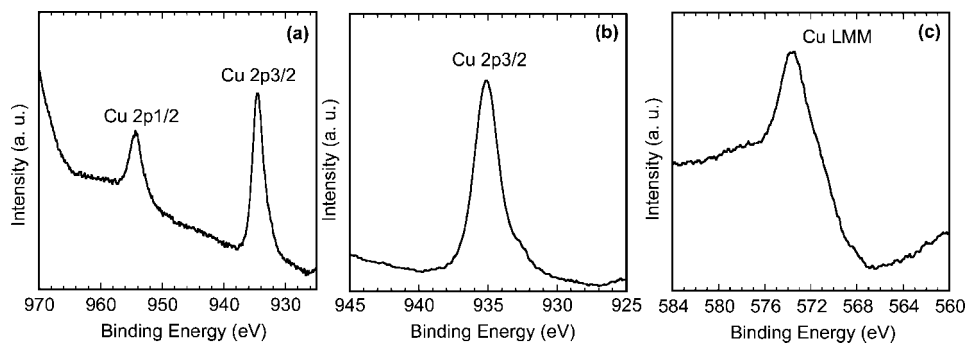


Figure 4. XPS spectra not corrected for charging effect of Cu 2p lines of (a) **C2** and (b) **C1** film and (c) Auger Cu_{LMM} spectra of **C1** film.

Table 1. XPS Data for **C2** and the **C1** Film

	C2					C1 film				
	BE values (eV)	BE Cu 2p _{3/2} corrected	correction	BE Values corrected (eV)	atomic %	BE values (eV)	BE Cu 2p _{3/2} corrected	correction	BE Values corrected (eV)	atomic %
Cu 2p _{3/2}	934.52	933	1.52	933	2.20	935.12	933	2.12	933	1.76
I 3d _{5/2}	621.24			619.72	2.56	621.75			619.63	1.78
P 2p	133.05			131.53	2.82	133.47			131.35	1.36
Si 2p	—					105.2			103.08	25.71
O 1s	532.14			530.62	30.76	534.9			532.78	27.23
C 1s	286.06			284.54	61.66	287.04			284.92	42.17

the film surface during the analysis or its transfer toward an UHV chamber. The Si 2p BE value of 103 eV for **C1** film is typical of SiO₂ sol–gel configuration with Si(IV) species. For the C 1s signal, the maximum BE values are slightly below 285 eV in agreement with the dominant phenyl contribution. The important result concerns the Cu 2p_{3/2} lines observed for the **C1** film with the total lack of shakeup satellite peaks characteristic of Cu(II) paramagnetic compounds (Figure 4), so the Cu(II) environment can be totally excluded. Even if the lack of Cu(0) is evident for synthesis consideration, the Cu(I) presence is totally confirmed by the Auger Cu_{LMM} line that is typical of a pure Cu(I) response, as expected for the studied clusters (Figure 4c). Note that a shoulder is observable in the Cu 2p_{3/2} line. This can be attributed to another Cu(I) specie. As the iodine signal is similar to the one observed for **C2** and because no Cu(II) species are present, we can suggest that the other Cu(I) species are structurally close to the cubane form [Cu₄I₄L₄]. A possible explanation is the distortion of the cubane form in the matrix. The cubane is four coordinated by phosphine bearing alcoxysilane groups. If all these groups are connected to the sol–gel silica matrix in the four directions, this generates constraints on the cluster and slightly changes the coordination environment of the copper. This phenomenon could explain the shoulder observed but needs to be confirmed by further investigations.

Optical Properties. At room temperature, clusters **C1** and **C2** emit intense yellow-green light under UV irradiation. Solid-state emission and excitation spectra of powder of **C2** are shown in Figure 5. At 295 K, the maximum of the emission band is observed at 570 nm ($\lambda_{\text{ex}} = 300$ nm). The external quantum yield of **C2** at room temperature is determined by using the standard luminophore Zn₂SiO₄:Mn as reference (Supporting Information). The quantum yield of **C2** is 64% under excitation at 260 nm. By lowering the temperature, a new emission band appears at higher energy, and at 87 K the two emission bands are clearly observed

with maxima at 425 and 572 nm. The excitation profiles are similar for the two emission bands.

Only qualitative luminescence study of **C1** cluster was done due to the difficulty of handling viscous oil. At room temperature, under UV excitation ($\lambda_{\text{ex}} = 300$ nm), **C1** exhibits a yellow luminescence centered at 585 nm. The thermochromic luminescence of **C1** is verified by a qualitative test. When the sample is immersed into liquid nitrogen, the luminescence becomes purple by irradiation at 312 nm. From previous studies on [Cu₄I₄L₄] (L = pyridine or amine derivatives) clusters, this thermochromism property appears to be specific to the cubane form. Thus, this luminescence behavior observed both for **C1** and for **C2** clusters also confirms their tetranuclear molecular structure. Moreover, the thermochromic luminescence property observed for **C1** and **C2** seems to be comparable to the one reported for [Cu₄I₄L₄] (L = pyridine or amine derivatives) clusters. In a first approximation, the similarity of the emission bands of **C2** suggests the same band assignment. The LE band at 572 nm could be assigned to a combination of an iodide-to-copper charge transfer transition (XMCT) and of a copper-centered d → s, p transition. The HE band at 425 nm could be attributed to iodide-to-phosphine ligand charge-transfer transition (XLCT). The presence of this band is in accordance

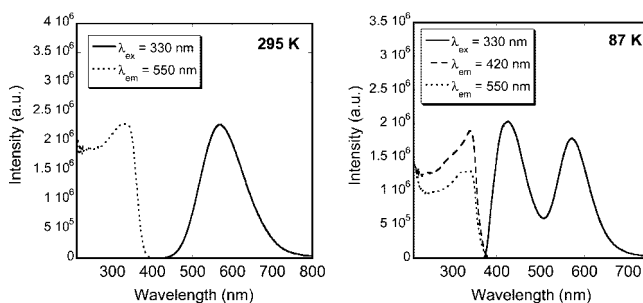


Figure 5. Solid-state excitation (dotted and dashed lines) and emission (solid lines) spectra at 295 and 87 K of **C2** powder.

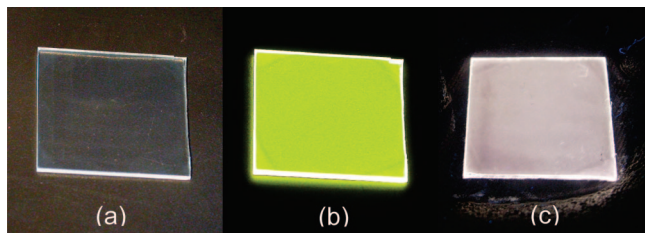


Figure 6. Photographs of **C1** film deposited on glass substrates ($1.5 \times 1.5 \text{ cm}^2$) (a) under ambient light and (b) under UV irradiation at 312 nm (UV lamp) at room temperature and (c) under UV irradiation at 312 nm (UV lamp) in liquid nitrogen.

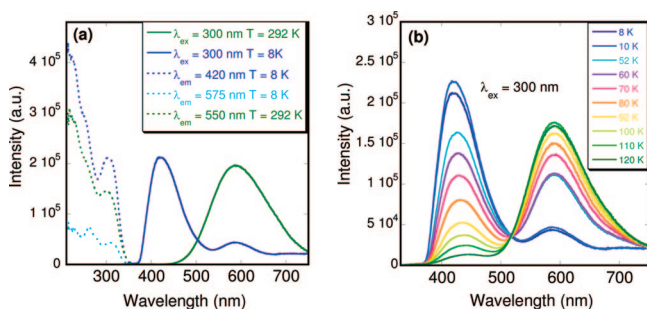


Figure 7. Temperature dependence of luminescence spectra for **C1** film on glass substrate (a) emission (solid lines) at 292 and 8 K with corresponding excitation spectra (dotted lines) and (b) emission spectra from 120 to 8 K with $\lambda_{\text{ex}} = 300 \text{ nm}$.

with the unsaturated character of the $\text{P}(\text{C}_6\text{H}_5)_2\text{C}_3\text{H}_7$ (**2**) and $\text{P}(\text{C}_6\text{H}_5)_2\text{Si}(\text{OC}_2\text{H}_5)_3$ (**1**) involved ligands.

Figure 6 shows the strong yellow emission of the hybrid colorless silica films obtained (**C1** film), under irradiation at 312 nm at room temperature. The internal quantum yield (Q) of **C1** film under excitation at 280 nm was evaluated to 31% by using a film of $\text{YVO}_4\text{:Eu}$ nanoparticles³⁴ as a reference (Supporting Information). This value is quite high and interesting for applications as light emitting devices, but it is worth noting that the wave-guiding effect of the light emission for the samples is not considered. As previously shown for **C1** clusters, thermochromic luminescence of films is revealed by immersion in liquid nitrogen. Under the same UV excitation, the yellow emission disappears and becomes purple (Figure 6c). It is clear that the observation of similar optical properties for clusters embedded in the sol–gel matrix also proves that a large part of them conserves their integrity in silica films.

The luminescence spectra of the films are recorded between 292 and 8 K and are shown in Figure 7. At 292 K, the emission spectrum of the **C1** film displays a single emission band centered at $\lambda_{\text{max}} = 589 \text{ nm}$. The emission wavelength is thus similar to the one observed for **C1** before its introduction in the sol–gel matrix ($\lambda_{\text{max}} = 585 \text{ nm}$) and is slightly shifted (19 nm) compared to **C2** ($\lambda_{\text{max}} = 570 \text{ nm}$). This band could be assigned to the LE band previously mentioned. As expected, at about 120 K, a new emission band appeared at 425 nm. By lowering the temperature down to 10 K, this band progressively increases in intensity with the concomitant extinction of the band at 589 nm. At 70 K, intensities of the two bands are similar and the addition of blue and yellow light gives the purple emission observed

for the film in liquid nitrogen (Figure 6c). This band could be assigned to the HE band discussed above attributed to a halide-to-ligand charge transfer emission (XLCT). Note that this band appears at a similar wavelength compared to the one observed for cluster **C2** ($\lambda_{\text{max}} = 425 \text{ nm}$) which has similar ligands. Moreover, the excitation spectra recorded for the LE emission at 292 K and for the HE emission at 8 K are quite similar with a maximum at $\lambda_{\text{max}} = 310 \text{ nm}$ (Figure 7a). When the sample is progressively warmed up to room temperature the yellow emission of the LE band is recovered, indicating a completely reversible thermochromism.

An important point is that in the 10–120 K range, all the emission curves present an isobestic point at 520 nm. This is characteristic of equilibrium of two thermally induced processes, which are in our case the light emission from the two LE and HE excited states. After integration of peaks, an Arrhenius plot leads to activation energy of 1760 J (150 cm^{-1}), corresponding to the difference between the energies of the two emission states in thermal equilibrium (Figure S4 in Supporting Information). In a comparable study, a higher value of 1000 cm^{-1} has been reported for the $[\text{Cu}_4\text{Br}_4(\text{dpmp})_4]$ (dpmp = 2-diphenylmethylpyridine) cluster.³⁵ This indicates a very high coupling of the two emissions states in our films.

Photophysical studies of the $[\text{Cu}_4\text{I}_4\text{L}_4]$ (L = pyridine or amine derivatives) clusters demonstrate marked environment sensitivity of the LE band with temperature but also with the rigidity of the medium.¹⁵ This rigidochromism behavior has been attributed to molecular distortions of the clusters.^{36,37} More recently, the position of the LE band has been reported to be directly related to the Cu–Cu distances in the cluster core $[\text{Cu}_4\text{I}_4]$.³⁸ According to theoretical works, the Cu–Cu bonds in the excited state (LUMO) are of bonding character. As the temperature decreases, the Cu–Cu distances become shorter, the bonding character increases, the energy level is lowered, and thus the LE emission band shifts to longer wavelength (from 580 nm at 298 K to 619 nm at 77 K for the $[\text{Cu}_4\text{I}_4\text{py}_4]$ cluster). In contrast, as observed for **C2**, no displacement of the LE emission band of **C1** film occurs by lowering the temperature from 295 to 8 K. This suggests no rigidochromism effect for sol–gel films and implies that Cu–Cu interactions are not involved in the LE emission band, which could be assigned to a pure XMCT transition without participation of copper transitions. In fact, the presence of the LE emission in our clusters and films could appear surprising because it has been previously suggested that only complexes with Cu–Cu distances less than twice the Van der Waals radius of Cu(I) (1.4 \AA) show the LE emission.¹⁵ This is clearly not the case for **C2** with Cu–Cu bond length average of 3.15 \AA . However, ab initio calculations at the Hartree–Fock level have clearly demonstrate a relationship between the Cu–Cu distances in the cubane type clusters and the energies and distortions (from the ground

(35) Ryu, C. K.; Vitale, M.; Ford, P. C. *Inorg. Chem.* **1993**, 32, 869.

(36) Vogler, A.; Kunkely, H. *J. Am. Chem. Soc.* **1986**, 108, 7211.

(37) Tran, D.; Bourassa, J. L.; Ford, P. C. *Inorg. Chem.* **1997**, 36, 439.

(38) Kim, T. H.; Shin, Y. W.; Jung, J. H.; Kim, J. S.; Kim, J. *Angew. Chem., Int. Ed.* **2008**, 47, 685.

(34) Huignard, A.; Gacoin, T.; Boilot, J.-P. *Chem. Mater.* **2000**, 12, 1090.

state) expected for the cluster centered (CC) excited states.³⁹ The reduced Cu–Cu interaction leads to less distortion in the CC state relative to the ground state. The lesser distortion leads to great communication with the XLCT state. While for the [Cu₄I₄(py)₄] pyridine cluster ($d_{\text{Cu–Cu}} = 2.69 \text{ \AA}$) the lowest energy excited state is such a CC state, the lowest excited state in the [Cu₄I₄(dpmp)₄] cluster (dpmp = 2-diphenylmethylpyridine, $d_{\text{Cu–Cu}} = 2.90 \text{ \AA}$) is a XLCT state. It seems that our clusters are likely to be a borderline case where the CC state is slightly separated from the XLCT state to be thermally populated from it. This leads to a high coupling between the two emissions at low temperature and a perfectly controlled thermochromic luminescence. Nevertheless, to verify the LE band assignment for **C2** and to elucidate the influence of the Cu–Cu interaction on this band, theoretical works and structure determinations are required for other phosphine-based clusters in relation with their luminescent properties. This will be the subject of further investigations.

Conclusion

Bright luminescent films under UV excitation based on copper-iodide clusters [Cu₄I₄L₄] have been synthesized using the sol–gel process. The incorporation of these new photoactive entities into the silica matrix was performed from their functionalization with phosphine ligands bearing alcoxysilane groups able to copolymerize with the MTEOS sol–gel precursor. By this way, the optical properties of these clusters are successfully preserved in the matrix. NMR and XPS analyses show that a great majority of the clusters remain intact in the film. Only some oxidized phosphine

ligands are detected in the film whose presence is inherent to the acidic sol–gel conditions. The use of other sol–gel matrixes involving different catalysis conditions could prevent this ligand oxidation.

To our knowledge, the clusters studied here are the first example of [Cu₄I₄L₄] clusters with L as phosphine ligand, which displays the thermochromic luminescence behavior. As a result of weak Cu–Cu interactions, the emissive states of [Cu₄I₄L₄] clusters with phosphine ligands appear as highly coupled with a low energy barrier ($2 \text{ kJ}\cdot\text{mol}^{-1}$). This leads to thermochromism in a large temperature range and contrasts with the prototypical [Cu₄I₄py₄] cluster for which the two excited states are weakly coupled with a higher energy barrier (about $10 \text{ kJ}\cdot\text{mol}^{-1}$).¹⁵ Photophysical studies of these phosphine-based clusters and especially correlation between structural and optical data should be investigated in the near future.

The luminescence properties of the sol–gel films display striking change in the color emission in temperature due to the cluster integrity. These films are the first exhibiting thermochromic luminescence, and they could be useful as sensors for numerous applications. They have the advantage of the relatively low cost and easy synthesis of the Cu(I) compounds. More generally, it appears that luminescent transition metal clusters constitute an interesting family of phosphors to investigate opening the way to original emissive materials.

Acknowledgment. The authors thank the CNRS for financial support and for the postdoctoral fellowship of C.T.

Supporting Information Available: The X-ray crystallographic file (CIF) and other characterization data (PDF). This material is available free of charge via the Internet at <http://pubs.acs.org>.

(39) Vitale, M.; Ryu, C. K.; Palke, W. E.; Ford, P. C. *Inorg. Chem.* **1994**, *33*, 561.